Ocean Systems Engineering, *Vol. 8, No. 4 (2018) 441-459*
DOI: https:// doi.org/10.12989/ose.2018.8.4.441

Coupled dynamic responses of a semisubmersible under the irregular wave and turbulent wind

Swarnadip Dey, Kaushik Saha, Pooja Acharya, Shovan Roy and Atul K. Banik*

Department of Civil Engineering, National Institute of Technology Durgapur, WB, India

(Received August 28, 2018, Revised October 27, 2018, Accepted November 5, 2018)

Abstract. A coupled dynamic analysis of a semisubmersible-type FOWT has been carried out in time domain under the combined action of irregular wave and turbulent wind represented respectively by JONSWAP spectrum and Kaimal spectrum. To account for the turbine-floater motion coupling in a more realistic way, the wind turbulence has been incorporated into the calculation of aerodynamic loads. The platform model was referred from the DeepCwind project and the turbine considered here was the NREL 5MW Baseline. To account for the operationality of the turbine, two different environmental conditions (operational and survival) have been considered and the aerodynamic effect of turbine-rotation on actual responses of the FOWT has been studied. Higher mean offsets in surge and pitch responses were obtained under the operational condition as compared to the survival condition. The mooring line tensions were also observed to be sensitive to the rotation of turbine due to the turbulence of wind and overestimated responses were found when the constant wind was considered in the analysis. Additionally, a special analysis case of sudden shutdown of the turbine has also been considered to study the swift modification of responses and tension in the mooring cables.

Keywords: FOWT; semisubmersible; irregular wave; turbulent wind; thrust force

1. Introduction

Wind energy harnessing presents a unique challenge to engineers and researchers worldwide, with a huge potential to setback the energy crisis which is arising due to the continuous depletion of fossil fuels. Considering the abundant wind availability, this, in turn, can be used to drive turbines for the generation of electricity without any toxic or heat-trapping emissions. In particular offshore wind enables the generation of higher power from fewer turbines due to greater wind speeds and causes lesser noise pollution than its onshore counterpart. From an economic perspective, primarily saving in cost for installation in deeper waters, floating wind turbines are more suitable than fixed type turbines. Thus, in recent years, a major focus has been directed towards the development of Floating Offshore Wind Turbines (FOWTs).

The most common approach for the design of floating wind turbines has been to design a support platform and adopting a commercially available wind turbine from the fixed offshore market. Tong (1998) was the first to conceptualize on the application of such floating offshore

*Corresponding author, E-mail: atul.banik@ce.nitdgp.ac.in

http://www.techno-press.org/?journal=ose&subpage=7 ISSN: 2093-6702 (Print), 2093-677X (Online)

platforms to the wind industry. He investigated the technical and economic aspects of wind farms and also proposed the design of a spar-buoy type FOWT called FLOAT. The engineering challenges that need to be overcome for the successful and economical deployment of FOWTs were highlighted by Musial *et al*. (2004) and Butterfield *et al.* (2005). They tried to classify the floating platforms on the basis of their static stability criteria and anchoring systems. Robertson and Jonkman (2011) carried out a comprehensive dynamic response analysis of different floating platform concepts supporting 5MW wind turbines. They reported that out of the platforms tested, the barge type floater shows maximum responses under wave excitation. Koo *et al.* (2014) and Goupee *et al.* (2014) have also presented an experimental comparison of three FOWT concepts focusing on global motions, tower dynamics, and mooring system loads. The semisubmersible type the floating platform has been identified as one of the suitable platforms for supporting a floating offshore wind turbine (Liu *et al*. 2016).

Harnessing of offshore wind energy at a viable cost for per unit of production requires a close interdisciplinary collaboration among researchers. From the point of view of global motions, the rotation of turbine blades influences the dynamic responses of a floating platform whereas the motions of the platform, in turn, affect the position and orientation of the turbine (Fig. 1) and consequently its aerodynamic performance (Collu and Borg 2016). The need for an integrated aero-hydro-servo approach in the design of FOWT model for dynamic analysis has been emphasized by Nielsen *et al.* (2006). Matsukuma and Utsunomiya (2008) studied the dynamic responses of a spar FOWT considering the rotor rotation, highlighting the effect of induced gyro-moment on the motions. The design requirements of a semisubmersible type FOWT called WindFloat is considered by Roddier *et al*. (2010) and Cermelli *et al.* (2009) with an aero-hydro model. The analysis was performed through wave tank tests and numerical simulations were carried out using the software package FAST. They concluded that the aero-hydro coupling of the turbine and floater requires thorough analysis and motion of the floater is required to be minimized for efficient operation of the turbine. Further, Karimirad and Moan (2012) presented a simplified method for coupled analysis of FOWTs considering both hydrodynamic and aerodynamic loads as against earlier works which were primarily carried out typically by the conventional aero-hydro-servo-elastic approach. Therefore, there is a need for an integrated approach to the analysis and design of FOWT.

Full-scale tests of FOWTs have been highly conservative in design to reduce the risks involved. The scale effects on small-scale model tests may be significant, rendering the tests potentially questionable in terms of their effectiveness as prediction tools for the full-scale behavior of FOWTs. That is why small-scale experiments may not always yield reliable results. The focus has been on the development of modeling and simulation tools for the analysis of FOWTs. To reduce the computational effort, often the researchers have adopted a frequency domain approach where a constant velocity wind has been considered in the analysis. A frequency domain approach is presented by Wang *et al*. (2017) for predicting the coupled responses of a semisubmersible-type FOWT including the turbine aerodynamics by means of a constant thrust force and a gyroscopic moment. A limitation of such a linear approach is that aerodynamic loads are not linear with wind velocity. Moreover, it has been noted that considering the wind speed variability due to turbulence can provide a more realistic prediction of the motions (Jamalkia *et al.* 2016).

In this paper, the coupled dynamic responses of a semisubmersible-type FOWT have been studied in the time domain, under the combined action of irregular wave and turbulent wind. The platform model for this study has been referred from the OC4 DeepCwind project while the turbine was the NREL 5MW Baseline. The validation of the model has been carried out by

comparing the natural periods from the free decay analysis and also by comparing the response amplitude operators (RAOs) from the wave excitation with those obtained through experimental works by Koo *et al*. (2014).

Variable wind speed data has been generated by the simulator TurbSim (Jonkman and Kilcher 2012), using Kaimal spectrum (Kaimal *et al.* 1972) with a turbulence intensity of 0.1. A time history of thrust force has been obtained from the wind speeds through a MATLAB code and was applied at the hub level of the turbine for the operating case whereas the gyroscopic moment generated has been considered in the damping matrix of the equation of motion of the system. In the analysis, irregular waves were represented by the JONSWAP spectrum for different sea states. The responses of the wind turbine and tensions in mooring cables have been obtained under the operational and survival environmental conditions (Koo et al. 2014) by means of operationality of the turbine by using hydrodynamic software package AQWA (ANSYS 2016). Additionally, a special analysis case of sudden shutdown of the turbine has also been considered to study the swift modification of platform responses and tension in the mooring cables.

2. Numerical modeling of a FOWT

2.1 Rigid body motion

For describing the motion behavior of the FOWT, a body-fixed reference axis was considered with its origin at the center of gravity and initially, it was parallel to the global reference axis, where the still water surface signifies the x-y plane while the z-axis points vertically upwards. In a time domain dynamic analysis of structure, a convolution integral form of the equation was used to account for the frequency dependent added mass matrix and damping matrix. The equation of motion as given in AQWA (ANSYS 2016) in wave frequency with slow drift may be represented as

$$\left\{\mathbf{M}+\mathbf{A}(\infty)\right\}\ddot{\mathbf{X}}(t)+\mathbf{c}\dot{\mathbf{X}}(t)+\mathbf{K}\mathbf{X}(t)+\int_0^t \mathbf{h}(t-\tau)\ddot{\mathbf{X}}(\tau)\partial\tau=\mathbf{F}_{hydro}+\mathbf{F}_{aero}+\mathbf{F}_{moor} \tag{1}$$

Here, **M** is the system mass matrix consisting of the mass component of the system and $\mathbf{A}(\infty)$is the added mass matrix component in infinite frequency; **c** is the linear frequency independent damping matrix, **K** is the system stiffness matrix consisting of the contributions from the hydrostatic stiffness, **X** is the displacement vector, $\dot{\mathbf{X}}$ is the velocity vector while $\ddot{\mathbf{X}}$ is the acceleration vector $\mathbf{F}_{\text{hydro}}$ includes the first order and second order wave excitation forces. $\mathbf{F}_{\text{aero}}$ is the aerodynamic forces. $\mathbf{F}_{\text{moor}}$ is the mooring dynamic force. Here, $\mathbf{h}(\tau)$ is the acceleration impulse function computed by the transform of the frequency-dependent added-mass matrix $\mathbf{A}(\omega)$ or hydrodynamic damping matrix $\mathbf{C}(\omega)$ in wave frequency ω is represented as given in AQWA (ANSYS 16)

$$\mathbf{h}(\tau)=\frac{2}{\pi}\int_0^\infty\left[\mathbf{C}(\omega)\frac{\sin(\omega t)}{\omega}\right]d\omega=\frac{2}{\pi}\int_0^\infty\left\{\mathbf{A}(\omega)-\mathbf{A}(\infty)\right\}\cos(\omega\mathrm{t})d\omega \tag{2}$$

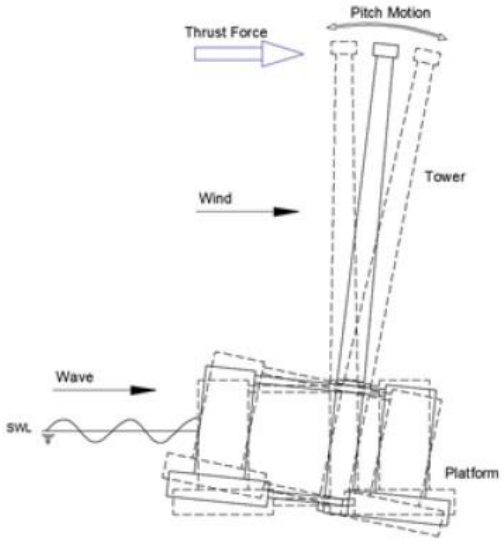

Fig. 1 Schematic diagram of FOWT under aerodynamic thrust

2.2 Hydrodynamic model

Hydrodynamic loading on a floating body is primarily caused by the kinematics of water particles in waves, resulting motions of the floater, and finally the interaction of structure and incident waves (Faltinsen 1990). Linear potential theory describes the water particle kinematics in terms of the incident wave potential as

$$\phi(x,z,t)=\frac{\eta_a g}{\omega}\frac{\cosh k(h+z)}{\cosh(kh)}\sin(kx-\omega t) \tag{3}$$

Here, $\omega/$ is the wave frequency, k is the wave number, η_a is the wave amplitude, h is the depth of water and g is the acceleration due to gravity.

Knowing the incident wave potential, a boundary element method was used to obtain the scattered wave potential. The large body surface was discretized into a number of diffracting and non-diffracting panels by AQWA (ANSYS 2016). These panels must not cut the mean water surface. All the panels not involved directly in the wave force calculation were referred to as non-diffracting panels. Thereafter, the wave forces were computed by integrating the pressures on the panel surfaces. Pressure distribution on the panels was obtained from linear Bernoulli equation considering both the incident and scattered wave potentials.

The platform motion has generated waves which exert a radiated force on the structure. Considering an appropriate body surface boundary condition a pressure field was generated. Integrating the pressure fields for six DOFs, a 6x6 radiated force matrix was obtained. One

component of this radiated force matrix is in phase with a velocity of the FOWT and acts as a damping term while another component which is in phase with the acceleration of the FOWT acts as an added mass term.

Apart from these, the structure is also subjected to second order difference frequency wave forces which are computed using a bi-chromatic diffraction theory. Quadratic Transfer Functions (QTFs) (Kim and Yue 1990) are generated for each pair of individual wave frequencies and a QTF matrix is obtained. Second order difference frequency load is calculated, for each pair of wave frequencies, as the product of incident wave heights and corresponding QTF component. The total load is obtained by summing over forces due to all such combination of frequencies. In the meantime, when a full calculation of QTF matrix is carried out, pressure on the wetted hull of the floating structure is integrated directly, correctly up to the second-order. All quadratic terms of the relevant boundary conditions are kept in a perturbation series.

Aqwa (ANSYS 2016) is unable to consider the wave viscous effect in a robust way. Although, an additional damping matrix was provided to delineate this effect. Viscous drag was taken into account by linearization and divided into constant force and damping, based on the equal energy dissipation between exact time domain analysis and linearized hull drag frequency domain analysis (Wang *et al.* 2017). After linearization, it can be integrated into Eq. (1) by panel method for larger hull and morison drag for column and braces. For the DeepCwind floating foundation, Robertson *et al.* (2014) presented the drag coefficients of different structures.

2.3 Aerodynamic model

Apart from the wind-induced wave, the wind itself makes an influential impact on motions of an FOWT system which has a significant wind exposed area above the water. In the present study, a unidirectional turbulent wind was acting in the same direction with the wave on the FOWT system. To realize the stochastic behaviour of the wind, an external tool TurbSim (Jonkman and Kilcher 2012) was used through which a time history of wind speed was generated. The turbulent wind speed is depending upon the specified turbulence intensity (0.1), a power spectral density of turbulence (Kaimal spectrum (Kaimal *et al.* 1972)) and a hub height mean wind speed. The analytical formulation of that IEC Kaimal model was referred from National Renewable Energy Laboratory (NREL) technical report by Jonkman and Kilcher (2012). The non-dimensional velocity component power spectrum S_k of IEC Kamial spectrum is given (Manwell *et al*. 2010, IEC-61400-3, 2009)

$$\frac{S_k(f)}{\sigma_k^{\,2}} = \frac{4L_k / \bar{u}_{hub}}{(1+6fL_k / \overline{u_{hub}})^{5/3}} \tag{4}$$

Here f is the frequency, k is the velocity component in three directions and L_k is the velocity component integral scale parameter. The wind speed time history graph with mean wind speed 11.5 m/s has been represented in Fig. 5.

2.3.1 Wind drag force

A nonlinear direct wind load, due to wind drag force and moment can be expressed in terms of a wind drag coefficient C_D and relative velocity term v. Using the averaged diameter (D_a) of NREL tower the drag force acting on the tower of height (H) is computed as follows:

$$F_D = \frac{1}{2} C_D \rho_a (D_a H) v|v| \tag{5}$$

Aqwa (ANSYS 2016) is based on potential theory and the drag coefficient C_D is obtained by means of experimental or Computational Fluid Dynamic or empirical approach under the condition of a known relative heading angle and known wind speed which were respectively constant and dynamic in the analysis. Under the condition of a known relative heading angle (β) and known wind speed (u), the force and moment about structure COG in the structure local axis frame are obtained by means of experimental or CFD or empirical approach, then the drag coefficients C_d at this specific heading angle can be converted by

$$F_D = \frac{1}{2} C_D \rho_a (D_a H) v|v| \tag{6}$$

2.3.2 Aerodynamic thrust force

Under the operating condition of the wind turbine, the rotor extracts kinetic energy of wind thereby decreasing the velocity of incoming airflow. To decrease the velocity of air the rotor exerts a force on the air and as a result, it itself experiences an equal and opposite thrust force in the downwind direction. The variation of thrust force with absolute wind speed for NREL 5MW turbine is shown in Fig. 7. In this paper, a time series of thrust force at hub level has been obtained from the turbulent wind speed data through a MATLAB code. This pre-calculated dynamic thrust force has been incorporated into the equation of motion as an external force, which was acting at a local reference system.

2.3.3 Gyroscopic moment

Apart from the thrust force, a gyroscopic moment also acts on the wind turbine while it is operating. The gyroscopic moment can be termed as rigid body-coupling between the turbine and floating platform. It arises because the rotating turbine is placed on a non-inertial floating foundation, which moves with respect to the inertial, earth-fixed, reference frame. Here, an additional frequency-independent damping matrix was considered to incorporate the gyro effect into the equation of motion of FOWT system and the damping values arising due to the gyro effect was obtained from the work of Tomasicchio *et al.* (2012).

Throughout the time analysis, the additional damping matrix acted in a global direction, was responsible for the yaw coupling with the pitch motion of the floating platform. This in part reflects the coupling effect between the floating foundation and wind turbine. Although, it was observed from previous study of Wang *et al*. (2017), that gyroscopic moments did not create any significant effect on responses for this type of semisubmersible platform. If I is the moment of inertia of rotor about surge axis, ω_r is the rotational velocity of rotor and Ω is the rotational velocity vector of the system the gyroscopic moment generated may be expressed as

$$M^g = I\Omega\omega_r \tag{7}$$

The gyroscopic force vector is then written as

$$F^g = (o, o, o, M_1^g, M_2^g, M_3^g) \tag{8}$$

2.4 Mooring dynamics model

As mooring lines are slender structures the mooring loads were not computed by diffraction theory. Thus, often a semi-empirical Morison equation was used which describes the load per unit length of cable as a sum of a drag term and an inertia term given as

$$dF_m = \frac{1}{2}\rho_w C_d D|u_r|u_r + \rho_w C_m \frac{\pi D^2}{4}\dot{u}_w - \rho_w \frac{\pi D^2}{4}(C_m - 1)\dot{u}_m \tag{9}$$

$$u_r = u_w - u_m \tag{10}$$

Here ρ_w is the density of water, C_d is the drag coefficient, C_m is the inertia coefficient, D is the diameter of mooring line, $\dot{u}_r$ and u_r are the transverse directional relative acceleration and the relative velocity between water particle velocity (u_w) and mooring body velocity (u_m)respectively. The forces on cable depend on the inertia and drag coefficients which were obtained either from lab experiments or from field tests and are dependent on the Keulegen Carpenter number and Reynold's number of the flow. Cable motion analysis was carried out including drag forces, elastic line tension, and bending moment coefficient. The motion of FOWT system under the action of irregular wave and the turbulent wind was also accounted for during the determination of forces on each cable element, thus providing a coupled solution.

2.5 FOWT model and properties

The semisubmersible model for the present study was referred from the OC4 DeepCwind project. The geometrical details of the model are shown in Figs. 2(a) and 2(b) whereas Table 1 shows the platform properties, supporting the wind turbine. The NREL 5MW Baseline was the reference turbine for which the properties were referred from Jonkman (2009). The model has been created in Design Modeler and imported into the Hydrodynamic Diffraction module of AQWA (ANSYS 2016) for analysis.

A 3D Panel discretization method (ANSYS 16.0) was used to discretize the platform body surface into a number of diffracting and non-diffracting panels. In carrying out meshing, the structure was divided into 9451 panels out of which 5727 panels were diffracting. The structure was considered as rigid and hence the flexible modes of the tower were neglected. The motions of the turbine-platform system were defined in terms of the displacement of its centre of gravity (0,0,-13.46) along the six degrees of freedom while the intersection of the water surface with the platform centreline served as the origin of the reference axes.

The configuration of mooring cables has been considered relative to the wave and wind direction as shown in Fig. 3. The mooring lines were modelled as catenary cables according to the data given in Table 2. Each cable was discretized using Morison elements and dynamics of the cable has been considered. A three-point Gaussian integration scheme was used for calculating forces on each element and the total loads were obtained by summation of individual forces and moments over all elements. Fig. 4 shows the platform-turbine mooring model as designed in AQWA (ANSYS 2016).

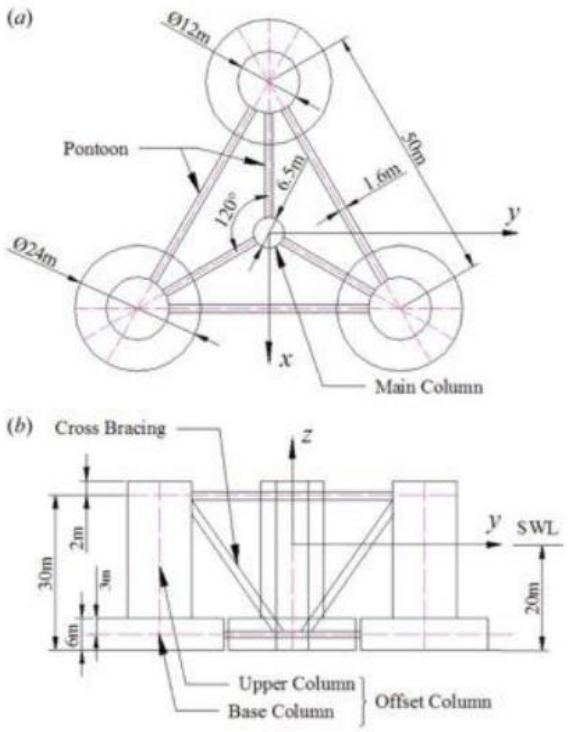

Fig. 2 (a) Plan and (b) side view of DeepCwind semisubmersible

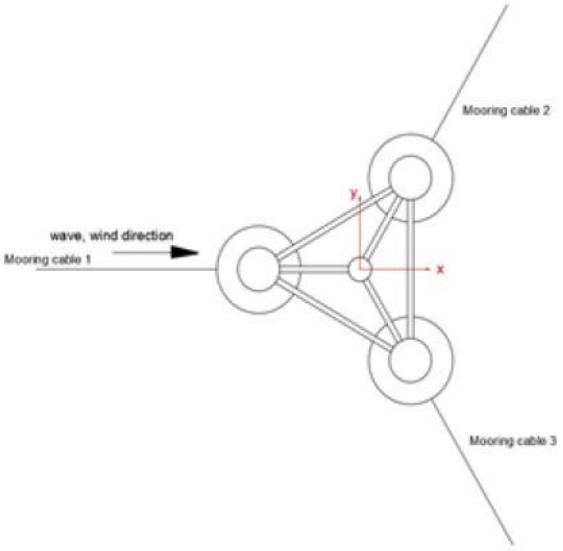

Fig. 3 The configuration of mooring cables

Table 1 Physical properties of DeepCwind semisubmersible

Structural parameter	Values
Draft	20 m
Platform mass, including ballast	1.3473 E+07 kg
CM location below SWL	13.46 m
Platform roll inertia about CM	6.827 E+09 kg-m^2
Platform pitch inertia about CM	6.827 E+09 kg-m^2
Platform yaw inertia about CM	1.226 E+10 kg-m^2

Table 2 Mooring line properties

Number of mooring lines	3
Angel between Adjacent Lines	120 degrees
Depth to Anchors Below SWL	200 m
Depth to Fairleads Below SWL	14 m
Radius to Anchors from Platform Centerline	837.6 m
Radius to Fairleads from Platform Centerline	40.868 m
Un-stretched Mooring Line Length	835.5 m
Mooring Line Diameter	0.0766 m
Equivalent Mooring Line Mass Density	113.35 kg/m
Equivalent Mooring Line Mass in Water	108.63 kg/m
Equivalent Mooring Line Extensional Stiffness	753.6 MN
Drag Coefficient for Mooring Lines	1.1
Sectional Added-mass Coefficient for Mooring Lines	1

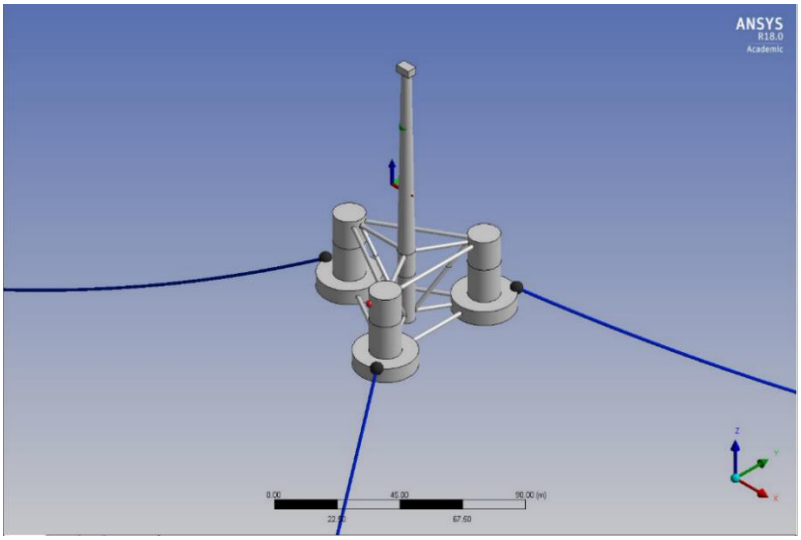

Fig. 4 FOWT model in AQWA (ANSYS 2016)

2.6 External loading parameters

The wind-driven wave parameters were selected based on data measurement in the offshore Gulf of Maine, mentioned by Koo *et al.* (2014). The JONSWAP spectrum was used to define the wave load in the undeveloped sea, on the structure and time input of its elevation (m) is shown in Fig. 6. Here, wind load was turbulent in nature with turbulence intensity 0.1 and followed Kaimal spectrum (Kaimal *et al.* 1972). To account for the operationality of the turbine, two different environmental conditions (operational and survival) have been considered (Table 3). The misalignment between wind blowing direction and wave heading direction of flow was ignored.

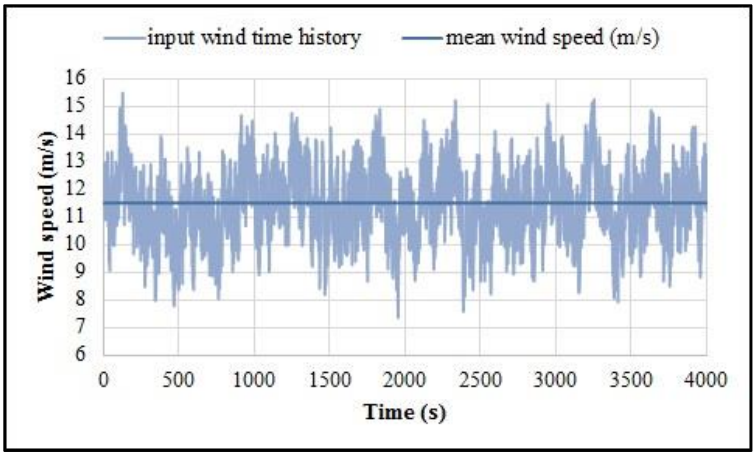

Fig. 5 Input wind speed time history (Kaimal spectrum with turbulence intensity 0.1 and mean wind speed 11.5 m/s

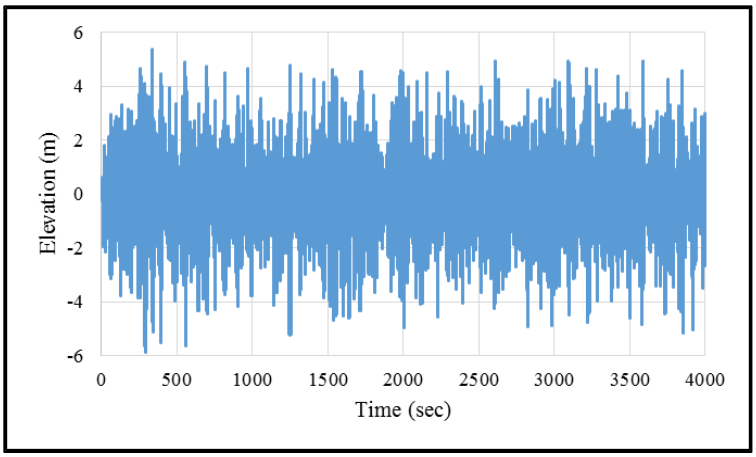

Fig. 6 Input wave elevation time history (JONSWAP wave)

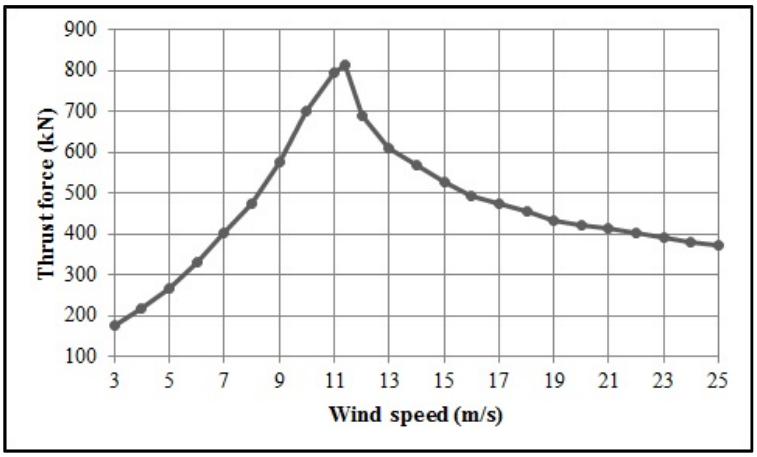

Fig. 7 Variation graph of thrust force in different wind speeds

Table 3 Selected wave and wind conditions (Koo *et al.* 2014)

Environmental condition	Sea state	Irregular JONSWAP spectrum			Wind state	Turbulent Kaimal spectrum
		H_S(m)	T_P(s)	Gamma		Mean speed
Operational	Moderate	7.1	12.1	2.2	Rated	11.5 m/s
Survival	Extreme	10.5	14.3	3.0	Cut out	35 m/s

Table 4 Comparison of natural periods from present study and Koo *et al*. (2014)

DOF	Present Study (Numerical model)	Koo *et al*. (2014) (Experimental model)
Surge	114.29	107.00
Sway	119.76	112.00
Heave	17.52	17.50
Roll	26.49	26.90
Pitch	26.43	26.80
Yaw	81.10	82.30

3. Validation of model

3.1 Natural periods

Free decay analysis of the structure has been carried out to obtain the natural periods. The natural periods thus obtained were compared with those reported by the work of Koo *et al.* (2014), which was experimental model test, performed at MARIN (Maritime Research Institute Netherlands) and the wind turbine was a scaled model of the NREL, 5MW horizontal axis reference wind turbine supported by a semisubmersible. A good match was observed as shown in Table 4.

3.2 Response Amplitude Operators (RAOs)

Figs. 8(a)-8(c) shows the comparison of Response Amplitude Operators (RAOs) obtained from regular wave test in the surge, heave, and pitch for the present study with those reported by Koo *et al.* (2014). The RAOs follow a similar pattern for the two cases thereby validating the present model. This signifies a good agreement has been made between the model presented in this paper and the model used in the work of Koo *et al*. (2014).

Aqwa (ANSYS 2016) solves a set of linear algebraic equations to obtain the harmonic response of the body to regular waves. These response characteristics are commonly referred to as response amplitude operators (RAOs) and are proportional to wave amplitude. It was assumed that each structure in a hydrodynamic interaction structure system is purely modeled by panel elements and freely floating. Hence, RAO was calculated by excluding the viscous effect as well as effect of mooring stiffness.

4. Results and discussion

In this paper, the coupled dynamic responses of the semisubmersible-type FOWT have been studied by following four different analyses (Table 5). They are,

Analysis 1: Effect of wind turbulence on responses
Analysis 2: Responses under parked and operating conditions of turbine
Analysis 3: Low Frequency and Wave Frequency responses
Analysis 4: Effect of sudden shutdown of turbine on responses

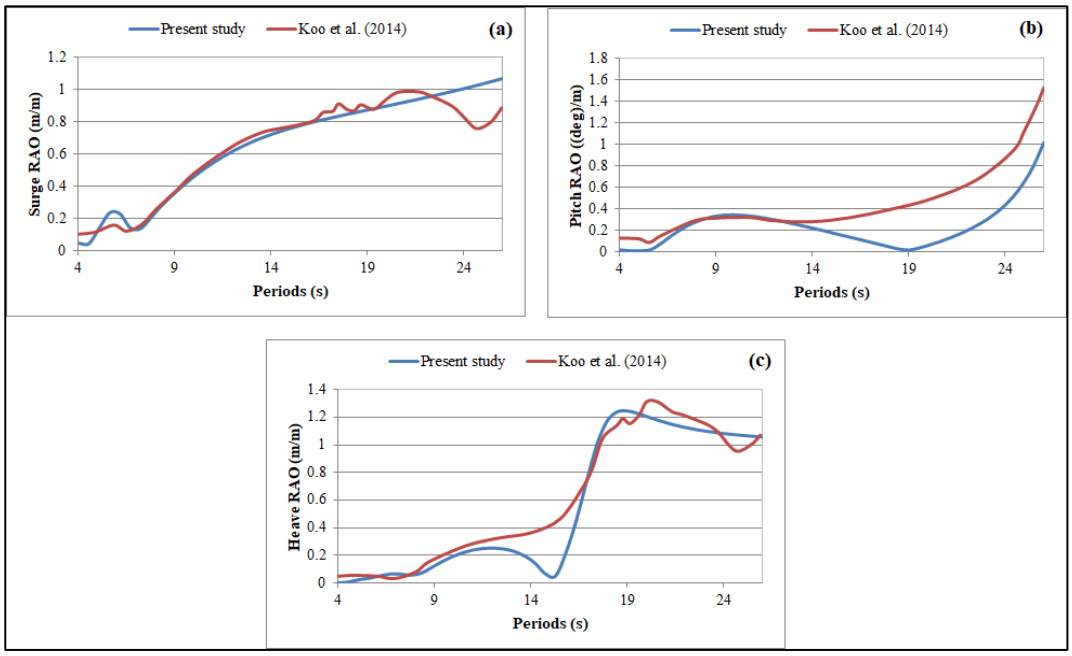

Fig. 8 RAO comparison. (a) Surge, (b) Heave and (c) Pitch

Table 5 External loading conditions in different analyses

Analyses	Environmental conditions	Sea state	Nature of wave	Wind speed	Nature of wind
Analysis 1	Operational	Moderate	Irregular	Rated	Turbulent
					Constant
Analysis 2	Operational	Moderate	Irregular	Rated	Turbulent
	Survival	Extreme		Cut-out	
Analysis 3	Operational	Moderate	Irregular	Rated	Turbulent
	Survival	Extreme		Cut-out	
Analysis 4	Sudden Shutdown	Moderate	Irregular	Rated	Turbulent

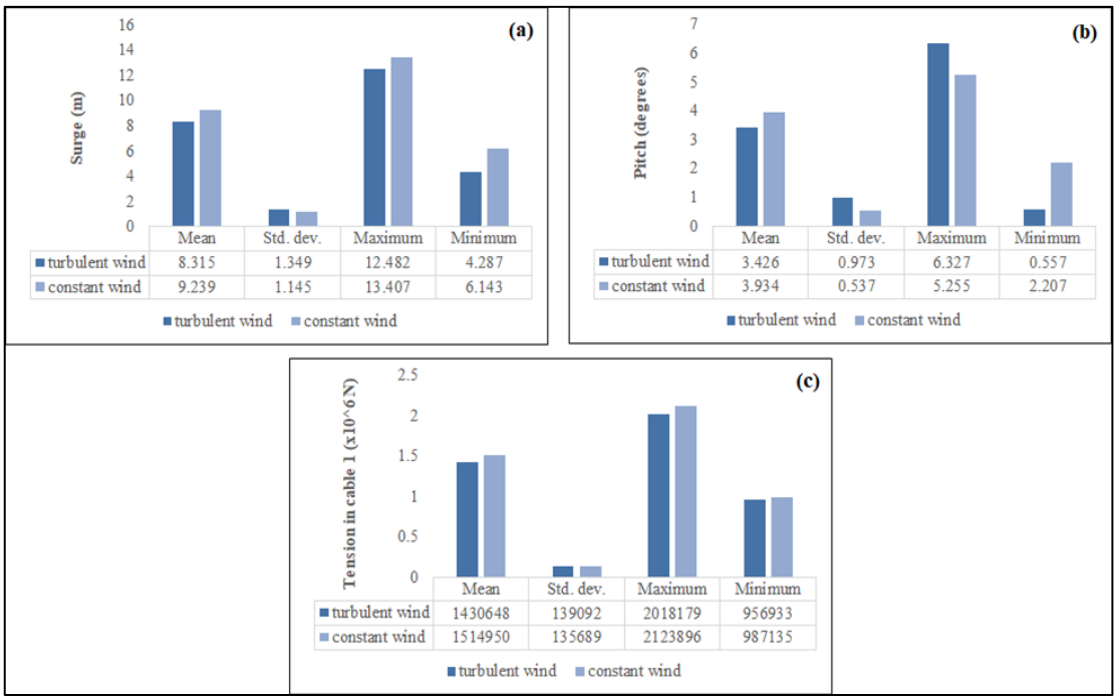

Fig. 9 Analysis 1: Statistical estimation of (a) surge responses, (b) pitch responses and (c) tensions in cable 1, under turbulent and constant wind load

4.1 Analysis 1: Effect of wind turbulence on responses

To investigate the effect of wind turbulence on the responses of the system, a constant wind analysis has been performed at the rated wind speed 11.5 m/s for the given wind turbine under operational condition. Figs. 9(a)-9(c) shows the mean, standard deviation, the maximum and minimum value of surge, pitch and cable 1 tension under the turbulent and constant wind

conditions. It was seen that neglecting the wind turbulence in analysis leads to an overestimation of the mean responses in surge and pitch as well as the mean tension in cable 1. This was because while carrying out constant wind analysis the wind speed is chosen is that for which the turbine experiences maximum thrust force. In reality, the mean of the dynamic thrust acting on the turbine was much lower (about 12.75%) than this value. Significantly, the standard deviations of responses were lesser by 15% in the surge and 45% in pitch when the wind turbulence was not accounted for in the analysis. Thus, for a more accurate and realistic prediction of the system responses, it is necessary to include the wind turbulence in the analysis of FOWTs.

4.2 Analysis 2: Responses under operational and survival conditions of turbine

The time histories of the surge, pitch responses, and tension in mooring line 1 under operational and survival conditions are presented in Figs. 10(a)-10(c). The mean offset in surge increases from 0.583 m in survival condition to 8.315 m in operational condition. Simultaneously, the mean offset in pitch increases from -0.058 degree to 3.427 degrees (Table 6). Yaw response does not assume significant values for either analysis case, although a slight increase in yaw is observed in operating condition due the effect of gyro-moment. The tension in line 1 has a mean value of 915 kN under survival condition which increases to 1430 kN under operational condition. Hence, the aerodynamic thrust force has produced significant mean offsets to the motions of the FOWT in all directions as well as upsurges the tension in the cable.

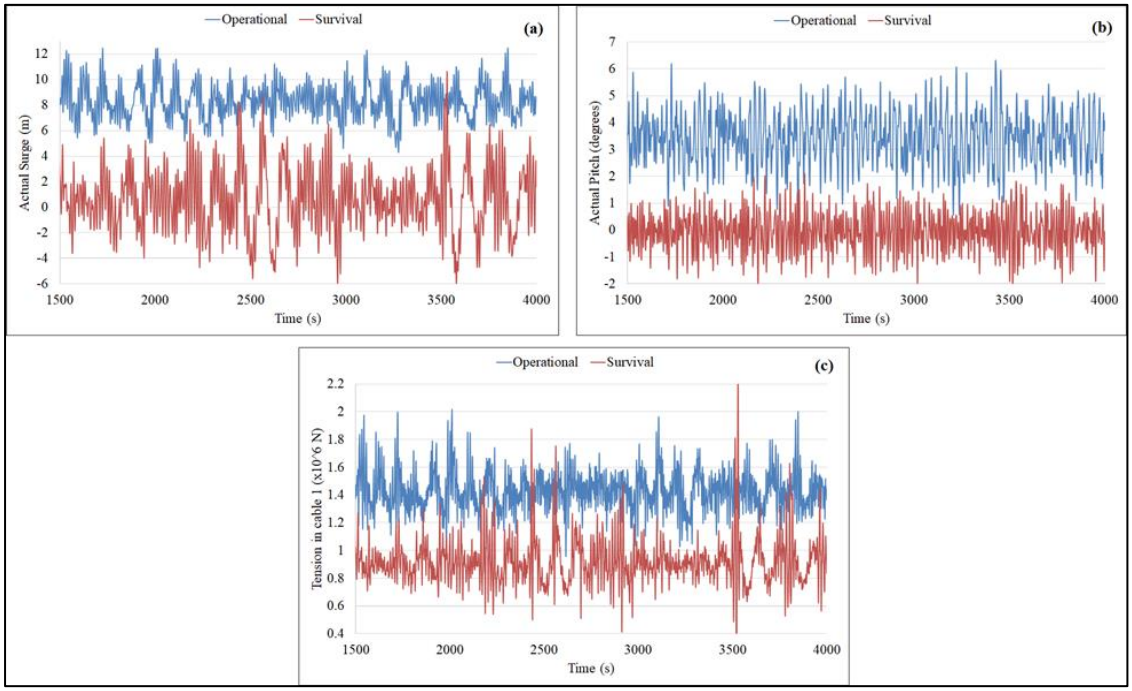

Fig. 10 Analysis 2: Time history of actual responses of FOWT under operational and survival conditions. (a) surge, (b) pitch and (c) tension in cable 1

Table 6 Statistical characteristics of motion responses under operational and survival conditions

Item	Characteristics	Operational	Survival
Surge (m)	Mean	8.315	0.583
	STD	1.350	2.445
	Max	12.500	10.600
	Min	4.290	-6.050
Pitch (degree)	Mean	3.427	-0.058
	STD	0.973	0.693
	Max	6.328	2.110
	Min	0.557	-2.252
Tension in Cable 1 (N)	Mean	1430648	915588
	STD	139092	160432
	Max	2018180	2282501
	Min	956934	140036

Whereas, the standard deviations of tension in cable 1 and surge responses seem to be increased in survival condition and more flattered responses are observed in operational condition. This is because of the extreme sea wave was acting in the surge direction. In the tested condition, the maximum pitch response reaches to value of 6.328 degrees, which is closer to the accepted limit of 10 degrees (Collu and Borg 2016). The pitch response is an important consideration since many of the turbine subsystems such as gearbox, bearing, generator etc. are designed to operate close to the upright condition of the turbine.

4.3 Analysis 3: Low frequency and wave frequency responses

The low-frequency subtype values were obtained by filtering the actual response with a filter which had a cut-off frequency; here 50 spectral lines were used in AQWA (ANSYS 2016). The wave frequency response is that which remains when the low-frequency response is subtracted from the actual response. Low Frequency and Wave Frequency surge and pitch responses under operational and survival conditions of the wind turbine were obtained in the time domain (Figs. 11(a)-11(d)). It was seen that the aerodynamic loads acting in the operational condition, the Low-Frequency surge and pitch responses causing a mean offset whereas the Wave Frequency responses are not much affected. As seen in Section 4.2, in operational condition, both the surge and pitch responses show an increased offset, which is due to the mean excitation of the structure. However, the Wave Frequency excitation in operational condition leads to an increased standard deviation of response in only the pitch degree of freedom while surge remains unaffected.

4.4 Analysis 4: Effect of sudden shutdown of turbine on responses

Failure of the components of the transmission chain of the turbine such as the hub, shaft, shaft bearing, gearbox, and generator may cause a sudden shutdown of the turbine. Such an occurrence may have a unique impact on the platform responses due to sudden transition from operating to the idle state of the turbine.

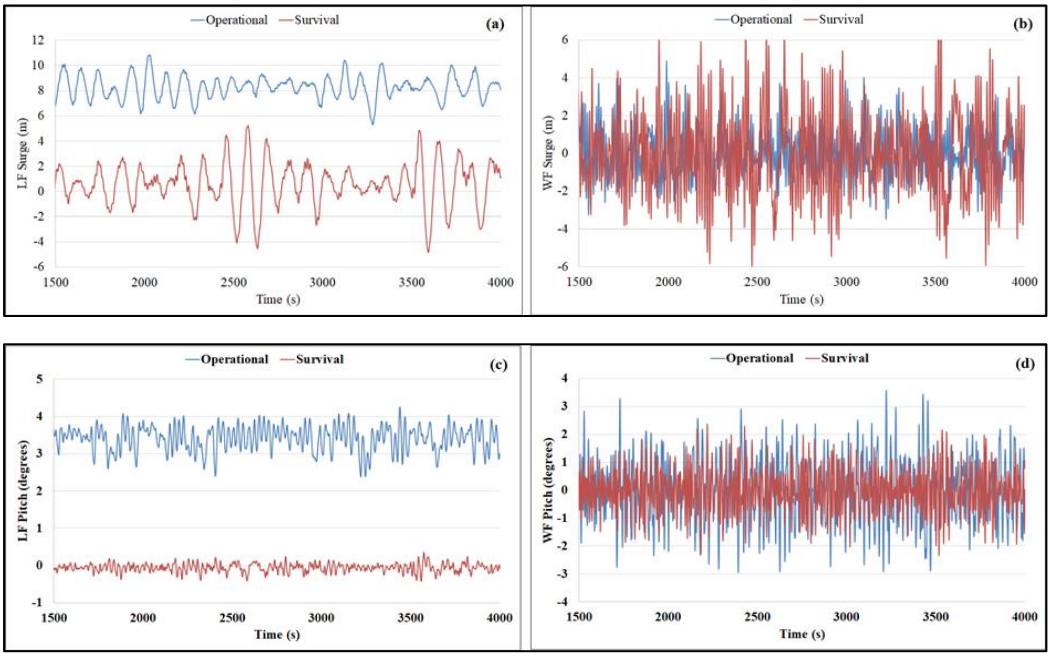

Fig. 11 Analysis 3: Comparison of (a) Low Frequency and (b) Wave Frequency surge responses and comparison of (c) Low Frequency and (d) Wave Frequency pitch responses, under operational and survival conditions

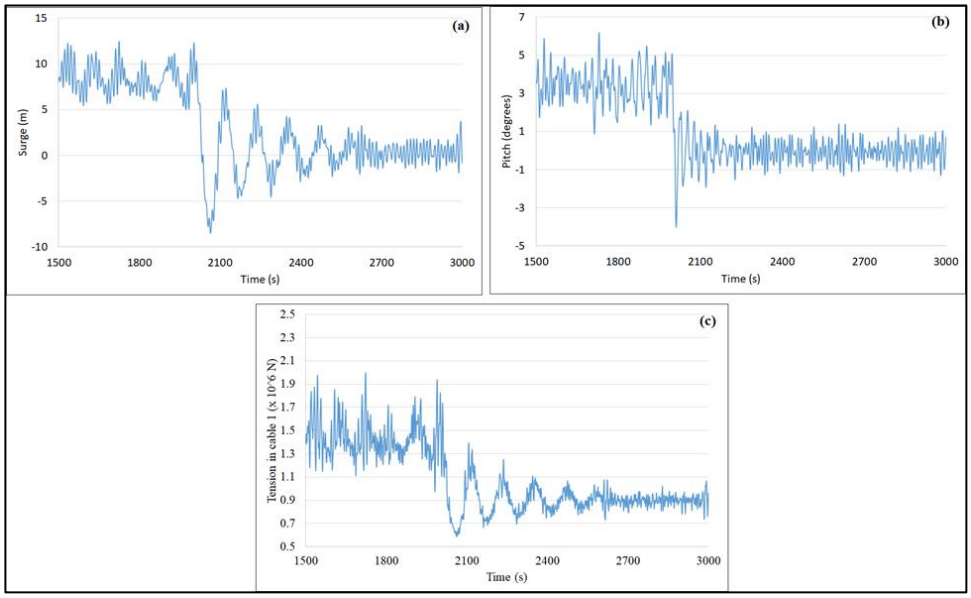

Fig. 12 Analysis 4: Time history of responses to special analysis case of sudden shutdown: (a) surge, (b) pitch and (c) tension in cable 1

The time histories of the surge, pitch and cable 1 tension in a sudden shutdown condition are shown in Figs. 12(a)-12(c). For this study, the sudden shutdown was considered to occur at the 2000s. It is observed that just after shutdown the Low-Frequency response dominates and maximum displacement was found in surge and pitch direction. During the transition, the system undergoes a global modification, which creates a transient motion, before going to new stationary states (different from the starting one). As a result, the transitory motion tends to mask the oscillatory motions induced by the existing excitations, because the transient motion is quite large compared with oscillations induced by environmental factors. The system motion in pitch direction attains stationary state in about 300s from shutdown whereas the motion in surge direction and cable tension reach this state much later at about the 2600s mark. This might be due to the fact that cable tension is significantly affected by surge motion. Significantly, a sudden drop in cable tension is also observed in such a circumstance.

5. Conclusions

In this paper, the dynamic responses of a semisubmersible-type FOWT have been analysed under the action of irregular wave and variable speed wind. The turbine aerodynamics has been incorporated into the analysis by means of a horizontal thrust force and a gyroscopic moment. The responses of the platform-turbine system have been studied in the time domain, under the operational and survival conditions. The effect of wind turbulence on the responses of the FOWT has been highlighted. Also, a special analysis case of sudden shutdown of the turbine has been studied. The major findings of this study are-

- Neglecting the wind turbulence, while calculating aerodynamic loads on the turbine, results in an overestimation of surge and pitch responses of the FOWT by 15% and 45% respectively.
- The FOWT responses are markedly different under the operational and survival conditions. In the tested condition, the maximum pitch response reaches the value of 6.328 degrees, which is closer to the accepted limit of 10 degrees (Collu and Borg 2016).
- In operational condition, both the surge and pitch responses show an increased offset, which is due to the mean excitation of the floater.
- If a sudden shutdown of the turbine occurs, a transition period is observed in surge and pitch responses, which is characterized by the mean excitation motion of the floater. The floater attains stationary in pitch much faster than in surge in case of such an occurrence.

The findings of this study emphasize the necessity of incorporating the turbulence of wind while considering the aerodynamic load in the analysis of integrated aero-hydro coupled analysis for a semisubmersible type FOWT. However, the additional platform pitch motion caused by the blade pitch control is not implemented here and the platform pitch motion can be underestimated in the operational condition (Kim *et al.* 2018). Also, the entire structure has been considered as rigid and hence the bending modes of the tower have been neglected. Thus, this study may be extended in the future to include the flexibility of tower and additional platform pitch motion in the response analysis.

References

ANSYS AQWA. (2016), AQWA user's manual release 17.0. USA. Canonsburg (PA): ANSYS Inc.

Butterfield, S., Musial, W., Jonkman, J., Sclavounos, P. and Wayman, L. (2005), "Engineering challenges for floating offshore wind turbines", *Proceedings of the Copenhagen Offshore Wind Conference*, 25 October- 27 October, Copenhagen, Denmark.

Cermelli, C., Roddier, D. and Aubault, A. (2009), "WindFloat: a floating foundation for offshore wind turbines part II: hydrodynamics analysis", *Proceedings of the ASME 2009 28th International Conference on Ocean*, Offshore and Arctic Engineering. American Society of Mechanical Engineers, 31 May-5 June, Honolulu, Hawaii, USA.

Collu, M. and Borg, M. (2016), Design of floating offshore wind turbines, Offshore Wind Farms Technologies, Design and Operation, (Eds., Chong Ng and Li Ran), 359-385.

Faltinsen, O.M. (1990), Sea loads on ships and offshore structures, Cambridge (UK): Cambridge University Press.

Goupee, A.J., Koo, B.J., Kimball, R.W., Lambrakos, K.F. and Dagher, H.J. (2014), "Experimental comparison of three floating wind turbine concepts", *J. Offshore Mech. Arct.*, **136**(2), 020906.

IEC 61400-1 (1999), "Wind turbine generator systems-Part 1: Safety requirements", 2nd Ed., Geneva, Switzerland: International Electrotechnical Commission.

Jamalkia, A., Ettefagh, M.M. and Mojtahedi, A. (2016), "Damage detection of TLP and Spar floating wind turbine using dynamic response of the structure", *J. Ocean Eng.*, **125**, 191-202.

Jonkman, J.M. (2007), "Dynamics modeling and loads analysis of an offshore floating wind turbine", NREL Technical Report No. TP-500-41958, November.

Jonkman, J.M. (2009), "Dynamics of offshore floating wind turbines model development and verification", *Wind Energy*, **12**(5), 459-492.

Jonkman, B.J. and Kilcher, L. (2012), TurbSim User's Guide: Version 1.06.00. Tech. Rep. DEAC36-08-GO28308, National Renewable Energy Laboratory, Golden, Colorado.

Kaimal, J.C., Wyngaard, J.C., Izumi, Y. and Cote, O.R. (1972), "Spectral characteristics of surface-layer turbulence", *Q. J. R. Meteorol. Soc.*, **98**, 563-589.

Karimirad, M. and Moan, T. (2012), "A simplified method for coupled analysis of floating offshore wind turbines", *Mar. Struct.*, **27**, 45-63.

Kim, H.C. and Kim, M.H. (2018), "The effects of blade-pitch control on the performance of semi-submersible- type floating offshore wind turbines", *Ocean Syst. Eng.*, **1**(6), 79-99.

Kim, M.H. and Yue, D.K.P. (1990), "The complete second-order diffraction solution for an axisymmetric body. Part 2. Bichromatic incident waves", *J. Fluid. Mech.*, **211**, 557-593.

Koo, B.J., Goupee, A.J., Kimball, R.W. and Lambrakos, K.F. (2014), "Model tests for a floating wind turbine on three different floaters", *J. Offshore Mech. Arct.*, **136**(2), 020907.

Liu, Y., Li, S., Yi, Q. and Chen, D. (2016), "Developments in semi-submersible floating foundations supporting wind turbines: A comprehensive review", *Renew. Sust. Energ. Rev.*, **60**, 433-449.

Manwell, J.F., McGowan, J.G. and Rogers, A.L. (2010), "Wind energy explained: Theory, design and application", 2nd Ed., Wiley, Sussex, England.

Matsukuma, H. and Utsunomiya, T. (2008), "Motion analysis of a floating offshore wind turbine considering rotor-rotation", *IES J. Part A: Civil Struct. Eng.*, **1**(4), 268-279.

Musial, W., Butterfield, S. and Boone, A. (2004), "Feasibility of floating platform systems for wind turbines", *Proceedings of the 42nd AIAA aerospace sciences meeting and exhibit*, 1007.

Nielsen, F.G., Hanson, T.D. and Skaare, B. (2006), "Integrated dynamic analysis of floating offshore wind turbines", *Proceedings of the 25th International Conference on Offshore Mechanics and Arctic Engineering*, American Society of Mechanical Engineers, 4 June-9 June, Hamburg, Germany.

Robertson, A.N. and Jonkman, J.M. (2011), "Loads analysis of several offshore floating wind turbine concepts", *Proceedings of the 21st International Offshore and Polar Engineering Conference*, International Society of Offshore and Polar Engineers, 19 June - 24 June 2011, Maui, Hawaii, USA.

Roddier, D., Cermelli, C., Aubault, A. and Weinstein, A. (2010), "WindFloat: a floating foundation for offshore wind turbines", *Renew. Sust. Energ. Rev.*, **2**(3), 033104-1-34

Tomasicchio, G.R., Armenio, E., D'Alessandro, F., Fonseca, N., Mavrakos, S.A., Penchev, V., Schuttrumpf, H., Voutsinas, S., Kirkegaard, J. and Jensen, P.M. (2012), "Design of a 3D physical and numerical experiment on floating off-shore wind turbines", *Proceedings of the 33rd Conference on Coastal Engineering*, 14 December, Santander, Spain.

Tong, K.C. (1998), "Technical and economic aspects of a floating offshore wind farm", *J. Wind Eng. Ind. Aerod.*, **74**, 399-410.

Wang, K., Ji, C., Xue, H. and Tang, W. (2017), "Frequency domain approach for the coupled analysis of floating wind turbine system", *J. Ship. Offshore Struct.*, **12**(6), 767-774.

MK